IEEE Access
Multidisciplinary | Rapid Review | Open Access Journal

Date of publication xxxx 00, 0000, date of current version xxxx 00, 0000.

Digital Object Identifier 10.1109/ACCESS.2017.Doi Number

The power-sharing system of DFIG-based shaft generator connected to a grid of the ship

Trong-Thang Nguyen, Member, IEEE, Duc-Minh Nguyen, and Quang-Vi Ngo

Faculty of Electrical and Electronic, Thuyloi University, Hanoi 11398, Vietnam

Corresponding author: Trong-Thang Nguyen (e-mail: nguyentrongthang@tlu.edu.vn).

This work was supported by Thuyloi University, Vietnam.

ABSTRACT This article proposes a control system for a ship power station using a doubly-fed-induction generator (DFIG). Firstly, the author analyzes the characteristics of the power generation system using DFIG based on the rotor sync signal technique and then proposes a control system for adjusting the active and reactive power of the generator supplied to the grid. The advantage of the rotor sync technique is that the two control channels of active and reactive power are independent. It is favorable for the author proposes the Fuzzy-PID controller for each control channel. The result is that active and reactive power always follow the desired values in a fast response time. Thus, the author applies this proposed system for automatic load division in parallel power grids on ships. The entire generator system has well ensured the load distribution between the shaft-generator and the grid in the case of changes in load consumption and rotor speed of the generator.

INDEX TERMS Shaft generator, Ship power station, Power-sharing, Main machine

I. INTRODUCTION

The shaft generator system on the ship was first introduced in 1982. After a short time, the company MAN B&W has studied its application possibilities. Since then, several shaft power generation models have been developed and applied in practice. Up to now, the shaft generator has been studied and involved a lot on ships. Through the survey, the ship owners and shipyards worldwide were entirely convinced by the benefits of using an integrated shaft generator than just arranging a single main engine for a propeller. Using the main engine to drive the generator combined with other generators is highly appreciated for technical and economic aspects. Especially with a large operating area at sea, shaft generators installed in the power station operates efficiently.

The ship's power requirement on the sea is only equal to 5-10% of the capacity of the main machine. Thus, the shaft generator takes advantage of the extra power to reduce the timeserving of the generators driven by diesel and reduce fuel consumption, so it increases the lifetime of other generators. Significantly, the power production cost of the shaft generator is only 50% of the diesel generator [1].

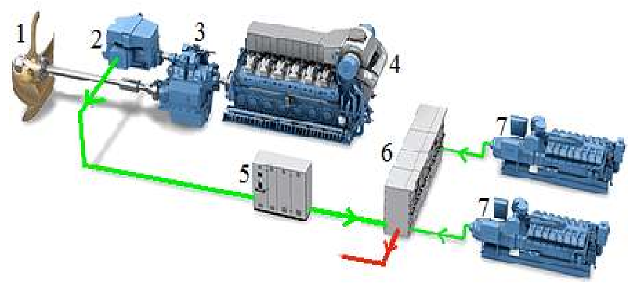

FIGURE 1. The ship's generation system with a shaft generator

The simplified diagram of the generator station on a ship using a shaft generator shows in Figure 1. The symbols are as follows: 1. Propeller; 2. Shaft generator; 3. Gearbox; 4. Main machine; 5. Shaft generator power controller; 6. Power distribution cabinet; 7. The diesel generators.

In Figure 1, the main machine is responsible for dragging the shaft generator and pulls the propeller. In this case, the ship's power station consists of a shaft generator working in combination with diesel generators.

However, the ship's grid is soft, the grid voltage changes frequently. Thus, connecting the generator to the grid is a complex mission for researchers [2, 3]. The challenging issue is controlling the shaft generator's voltage equal to the ship's unstable grid voltage when changing the main engine

This article has been accepted for publication in a future issue of this journal, but has not been fully edited. Content may change prior to final publication. Citation information: DOI 10.1109/ACCESS.2021.3102659, IEEE Access

speed [4, 5]. Moreover, the capacity of the main engine is hefty compared to the electric generator, so the rotor speed of the generator only depends on the speed of the main machine. Hence, the speed range of the generator rotor is extensive.

Thus, the author proposed the generator based on a doubly-fed induction machine because this generator can keep the stable frequency of output voltage while changing the rotor speed [6, 7].

Almost of researches on DFIG [8, 9] used the space vector modulation method. In these methods, firstly, the voltages and currents of the rotor and stator transform to the stator-flux-orientated coordinate or the grid voltage-orientated coordinate [10, 11] for calculating and controlling. Finally, all the voltages and currents transform to the stator or rotor frame. Therefore, the system must include two transmission stages of coordinates. It makes the structure of the control system more complex.

The author has proposed a new method that does not need the transmission stage of coordinates [12]. Instead, the rotor signals of the small DFIM are an initial signal for controlling the rotor current fed into the DFIG. Although this study just proved the feasibility of the model by mathematical equations and gave a single generator model, the results have not yet been applied in parallel power generation systems, especially in the division of electric supply on ships.

In this research, the author will apply the rotor-sync signal-based DFIG to the shaft generator of the ship. Then, controlling the power of the shaft generator fed into the grid reaches the desired values.

The most common controller is the PID with a simple algorithm and high robustness, but the adaptability is low. Each set of parameters of the PID controller is only suitable for a specific object and situation. Some algorithms are applied to achieve the optimal global parameters of the PID controller, such as genetic algorithm and particle swarm optimization. Still, the disadvantage is reducing noise compensation efficiency and reducing the dynamic qualities [13]. One method with fast response is the sliding mode controller, but the system has high-order harmonics. The advanced method recently improved Model Predictive Current Control [14], which defines the optimal values based on the direction of the current track in the established reference frame. This method has reduced the harmonics effectively. The research [15] combines the Model Predictive Control with a sliding-mode disturbance observer. It has reduced the calculation complexity of the observation value for the nonlinear model and improved the current reference accuracy. The research [16] has proposed a state feedback controller based on a grey wolf optimization algorithm, has improved computational efficiency, and suppressed overshoot.

Besides, some intelligent controllers are introduced, such as Fuzzy logic control [17], Neural-network-based control [18]. These methods can control fast the object with difficulties controlling. For example, the objects have the characteristic of nonlinearities, underactuated, dead zone, and uncertainties. Moreover, these control systems are highly adaptable and robust.

To take advantage of the different controllers, we proposed a combination of PID controller and Fuzzy logic that call Fuzzy-PID controller. The PID controller has high robustness, its parameter adjusted by the Fuzzy logic controller to increase the adaptability. We will apply the combination of these controllers to control the generator's active power and reactive power fed into the grid. Then, using the result to share the load of the ship grid.

Therefore, in this research, we will address the following problems:

- Proposing the sync-signal-based generator using DFIG. The outstanding advantage of the solution is to eliminate complicated calculation stages, making the system simple and easy to fabricate.
- Design of the control system for controlling the power components of the generator fed into the grid.
- Finally, we build the power-sharing system of electrical distribution on the ship.

II. THE CONTROL SYSTEM OF THE DFIG-BASED SHAFT GENERATOR

DFIG is the doubly-fed induction machine used in the generator mode. The structure of DFIG used in the parallel grid shows in Figure 2. It has windings in both stator and rotor. The electric powers generated on the stator (P_s, Q_s) can feed directly to the grid. The power control circuit is located in the rotor, includes the rotor side control and the grid side control. Therefore, the powers of the control circuit (P_r, Q_r) are small compared with the generated powers. Moreover, this generator can keep the stable frequency of output voltage while changing rotor speed. Because of these advantages, the generator using DFIG accounts for 50% of the wind power market.

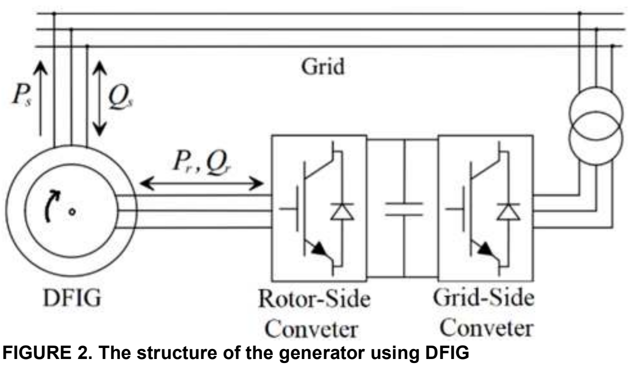

FIGURE 2. The structure of the generator using DFIG

There are some techniques for controlling the DFIG. The static Scherbius with the structure such as current-fed dc-link converter or cyclo-converter [19]. But these structures produce high order harmonics at the rotor current and induced stator. The common methods are all designed based on space vectors. All these methods must have two coordinate transition stages, so the calculation process and controlling are complicated.

This article has been accepted for publication in a future issue of this journal, but has not been fully edited. Content may change prior to final publication. Citation information: DOI 10.1109/ACCESS.2021.3102659, IEEE Access

Therefore, the author proposes a new model of shaft generator using DFIG based on the rotor sync signal as Figure 3. It includes:

- The main machine has the role of pulling the propeller. In addition, through the gearbox, its function is to move the shaft generator.
- DFIM with the rotor attached to the high-resistance and the stator emits the power. The rotor signal is the initial unit for creating the signal to control the DFIG.
- An isolation stage has the input with high resistance.
- The current control circuit has the role of creating the current with a value equals to the value of input voltage.
- DFIG is the generator that emits electric power.

We fasten the rotors of the two electric machines.

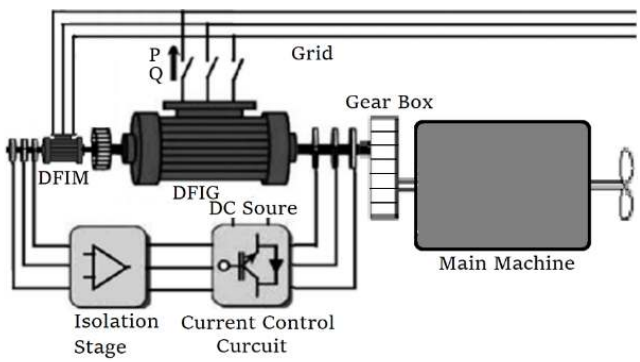

FIGURE 3. The shaft generator using DFIG based the rotor-sync-signal technical

The system consists of two machines, so we name the parameters: ${}^{M}X$ for DFIM and ${}^{G}X$ for DFIG. For example, ${}^{M}L_s$ is the stator inductance of DFIM and ${}^{G}L_s$ is the stator inductance of DFIG.

In the grid voltage-orientated coordinate, the q-component of the stator voltage ${}^{G}u_{sq} = 0$, so the active and reactive powers of the DFIG stator are as following [8, 20]:

$$P = (3/2).\ {}^{G}u_{sd}.\ {}^{G}i_{sd} \quad (1)$$

$$Q = (3/2).\ {}^{G}u_{sd}.\ {}^{G}i_{sq} \quad (2)$$

With ${}^{G}u_{sd}$ denotes the d component of the stator voltage, ${}^{G}i_{sd}$ and ${}^{G}i_{sq}$ denote the d and q components of the stator current, respectively.

In research [12], we have:

$${}^{G}i_{sd} = -({}^{G}L_m/\ {}^{G}L_s)\ {}^{G}i_{rtd} \quad (3)$$

$${}^{G}i_{sq} = -({}^{G}L_m/\ {}^{G}L_s)\ {}^{G}i_{rtq} \quad (4)$$

With ${}^{G}L_m$ and ${}^{G}L_s$ denote stator and mutual inductance, respectively.

$${}^{G}i_{rtd} = G_p.\ {}^{G}i_{rd0} \quad (5)$$

$${}^{G}i_{rtq} = G_q.\ {}^{G}i_{rq0} \quad (6)$$

Where: ${}^{G}i_{rq0}$ is created by ${}^{G}i_{rq0} = -\ {}^{G}\underline{i}_{r0}^{f}$, and ${}^{G}i_{rd0}$ is created by rotating the vector ${}^{G}\underline{i}_{r0}^{f}$ with an angle of $\pi/2$. With ${}^{G}\underline{i}_{r0}^{f}$ denotes the current vector of the DFIG rotor on the grid voltage-orientated coordinate. It is the adjusted value for satisfying all conditions for connecting DFIG to the grid. For more detail, on the grid voltage-orientated coordinate, the vectors as Figure 4.

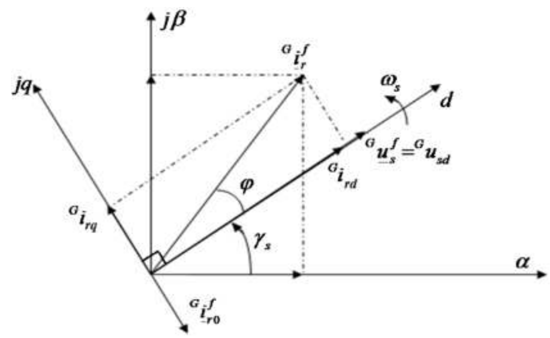

FIGURE 4. The DFIG rotor current vectors

According to equation (1-6), we obtain equations of the DFIG stator powers fed into the grid as follows:

$$P = -(3/2).G_p.\ {}^{G}u_{sd}.\ {}^{G}i_{rd0}.({}^{G}L_m/\ {}^{G}L_s) = G_p.X \quad (7)$$

$$Q = -(3/2).G_q.\ {}^{G}u_{sd}.\ {}^{G}i_{rq0}.({}^{G}L_m/\ {}^{G}L_s) = G_q.Y \quad (8)$$

Where: ${}^{G}i_{rd0}$ and ${}^{G}i_{rq0}$ denote the d and q components of the rotor current vector in the grid voltage-orientated coordinate.

In the grid voltage-orientated coordinates, ${}^{G}u_{sd}$, ${}^{G}i_{rd0}$, ${}^{G}i_{rq0}$ are constant. Thus, X and Y are constant. We can control the active and reactive power separately by adjusting Gp and Gq. The structure of the control system is as Figure 5.

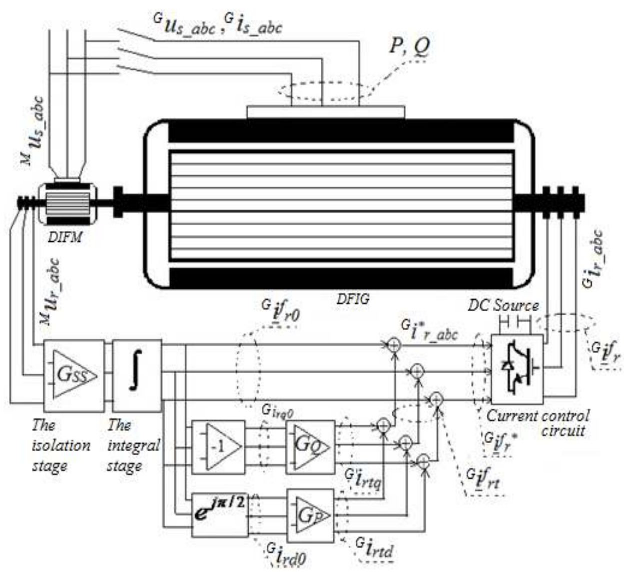

FIGURE 5. The system diagram of DFIG using rotor sync signal method

This article has been accepted for publication in a future issue of this journal, but has not been fully edited. Content may change prior to final publication. Citation information: DOI 10.1109/ACCESS.2021.3102659, IEEE Access

The system includes the following stages:

- The isolation stage.
- The integral stage
- The current control circuit
- The $e^{j\pi/2}$ has the role of rotating the signal with the angle of $\pi/2$.
- The amplitude coefficients Gq and Gp.

Considering the equations (7, 8), we can adjust the active and reactive power independently by changing the amplitude coefficient G_P and G_Q.

For the shaft generator to connect to the ship grid, the first requirement is that the generator voltage has an equal frequency, amplitude, and phase to the grid voltage. The following requirement is to control the active and reactive power fed into the ship grid independently according to the consumption load of the ship. In the shaft power generator systems using DFIG with rotor-sync signal technique, the first condition is always satisfied [12]. Therefore, the remaining problem is setting up the control system for controlling the power components emitted to the ship grid according to the desired values.

Based on equations (7, 8), the control mission of active and reactive power channels fed into the grid is very convenient. The active power is in proportion with the d component of the rotor current ($^2i_{rd}$), the reactive power is in proportion with the q component of the rotor current ($^2i_{rq}$). These components are modulated based on the rotor sync signal. The amplitudes of $^2i_{rd}$, $^2i_{rq}$ can be adjusted through the amplitude coefficient G_P and G_Q. Therefore, we can control the active and reactive power fed into the grid through these amplitude coefficients. Next, the author will design the control system for the power components of the shaft generator.

III. BUILDING THE CONTROL SYSTEM

A. IDENTIFYING THE CONTROL OBJECT STRUCTURE

Before building the control system, the first mission is to identify the control object structure, which means identifying the suitable input and output for control convenience. The system structure of the shaft generator using DFIG includes many units such as the doubly-fed induction machine (DFIG1), doubly-fed induction generator (DFIG2), the grid-side converter, the machine-side converter, the signal processors, the intermediary DC circuit, etc. Therefore, it is difficult to identify the control object model. To control the system effectively, we must consider the control mission for choosing the control output, then place the suitable control input.

The author identifies the control object that includes two independent control channels shown in Figure 6. The first channel controls the d component rotor current of DFIG2 ($^2i_{sd}$), with its input is coefficient G_P, and its output is the $^2i_{sd}$ (proportion with the active power P). The second channel with the role of controlling q component rotor current of DFIG2 ($^2i_{sq}$), the input is coefficient G_Q, the output is the $^2i_{sq}$ (proportion with the reactive power Q).

A sensor measures the active and reactive powers of the load (P_L, Q_L). After the load sharing calculation, we have the desired value of generator powers fed into the grid (P^*, Q^*). The mission of the control system is to control the generator power components follow the desired values (P^*, Q^*).

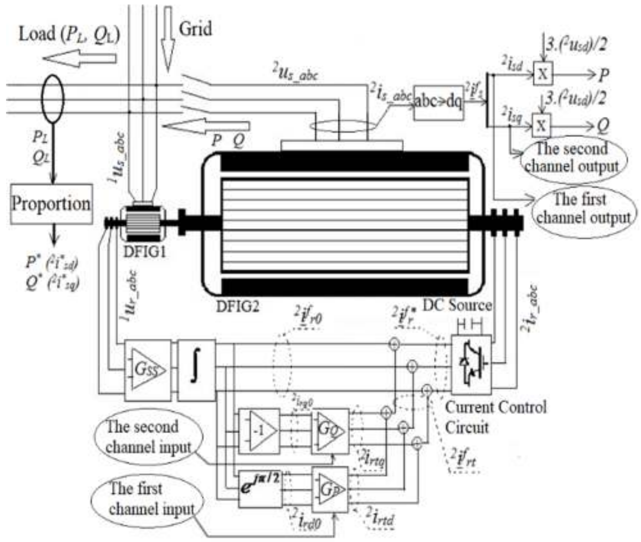

FIGURE 6. The control object

With the proposed control object, each control channels are independent. The simplified control object is as Figure 7.

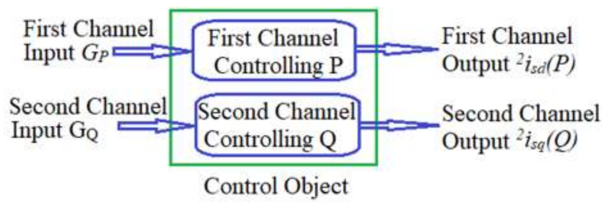

FIGURE 7. The simplified control object

B. DESIGNING THE FUZZY-PID CONTROLLER

The combination of PID controller and Fuzzy logic takes advantage of each controller to produce the control system with high adaptive and robustness.

The control system is as Figure 8. The control object includes two independent power channels: the active power channel and the reactive power channel. Each track is controlled by a PID controller with its parameters (*KP, KI, KD*) adjusted by the Fuzzy controller using the Madani model [21, 22].

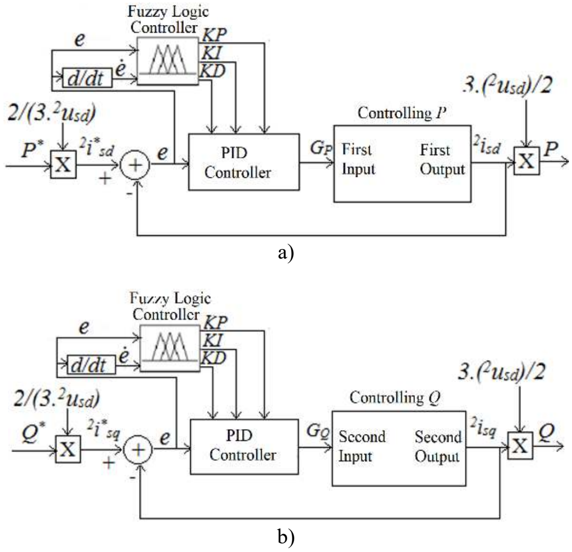

FIGURE 8. The control system of power components by the Fuzzy-PID controller

In the active power channel P, the Fuzzy logic adjusts the parameters of the PID controller. The input of the Fuzzy controller includes the error e and derivative of error $\dot{e}$. The output of the Fuzzy controller contains the values of *KP, KI, KD*.

The author designs the Fuzzy controller for adjusting the parameter *KP, KI, KD* based on the experiment. Next, the author will build the Fuzzy controller.

Choosing the membership function: Firstly, we must define the Fuzzy set for the input and output variables. With the characteristic of this object, the author sets the number of each input and output variable equal to 5. Generally, the language number of each variable is about 3-10. If the number is small, the relationship of input-output is not detail and unuseful for practice. If the number is too large, the association of input-output is too smooth, and it is too difficult to set up all of the cases. Moreover, it needs the large memory of the program, so it makes the processing speed slower.

Secondly, we chose the shape type for membership functions. There are many shape types such as *Gaussian, PI-shape, S-shape, Sigmoidal, Z-shape*. It is essential to select a suitable type of membership function. Based on the characteristic of the object, the author chose a triangle shape. Because this shape presents the relationship between the Fuzzy set with each input value clearly and it is easy to program in the controller.

Based on the above analysis, the author chooses membership functions of inputs e and $\dot{e}$ shown in Figure 9.b. Each input value includes five language values such as Negative Big (NB), Negative (N), Zero (Z), Positive (P), and Positive Big (PB). Its range is [-1 1] pu.

Next, we choose the output membership functions *KP, KI, KD* shown in Figure 9.c. Each output value includes five Fuzzy sets such as Very Small (VS), Small (S), Medium (M), Big (B), Very Big (VB). Its range is [0 1] pu.

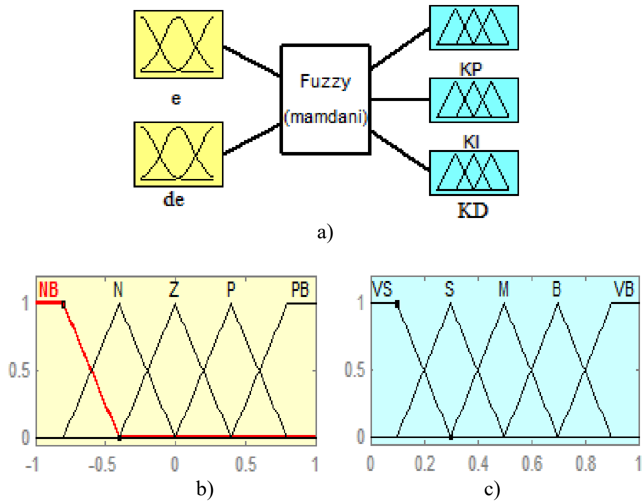

FIGURE 9. The Fuzzy logic controller and membership function

The inference laws are built based on the characteristic of the object and the experiment [23]. Based on the response of the loop system in case of changing the parameters *KP, KI, KD* [24, 25], and the characteristic of the control object, we propose the inference laws presented in Table 1.

TABLE I

The inference laws of fuzzy controller

K_P, K_I, K_D		e				
		NB	N	Z	P	PB
	NB	VS/VB/VS	VS/VB/VS	VS/VB/VS	S/S/B	M/VS/VB
	N	VS/VB/VS	S/B/S	S/B/S	S/M/M	M/VS/VB
$\dot{e}$	Z	VS/B/S	S/B/S	M/M/M	B/S/B	VB/VS/VB
	P	M/B/S	B/M/M	B/S/B	B/S/B	VB/VS/VB
	PB	M/M/M	B/S/B	VB/VS/VB	VB/VS/VB	VB/VS/VB

Setting the composition rule is Min-Max type, defuzzification by the centroid method. Finally, we have the graphs of the relationship of the input and output variables shown in Figure 10.

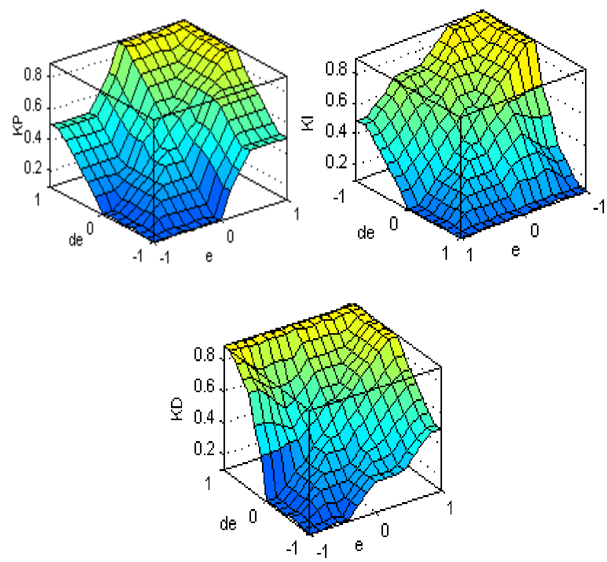

FIGURE 10. The relationship of the input and output variables of the Fuzzy controller

Next, we design the controller for the reactive power Q. this process is similar to the channel of active power P Because the reactive power channel Q has the same characteristic as the active power channel P.

We run the overall system in the case of changing the desired values (P^*, Q^*) as following: the initial time, $P^*=Q^*=0$, then we change the values of P^*, Q^* at the time of *1.4s, 1.6s, 1.8s, 2.0s,* and *2.2s*. The results show in Figure 11.

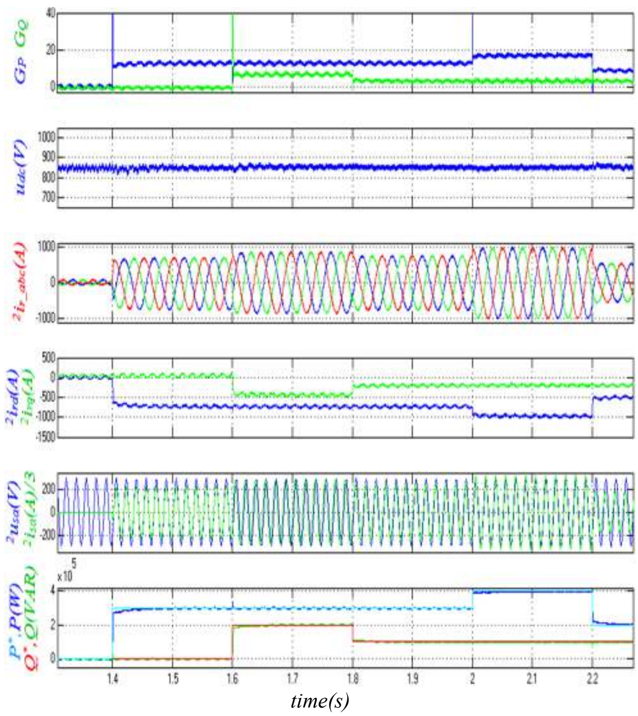

FIGURE 11. The results of the control system with the Fuzzy-PID controller

The results show that the values of the active and reactive power (P, Q) of the DFIG2 stator always follow the desired values (P^*, Q^*) with the short transition time (about 0.001s) and none of the overshoot. Considering some of the previous research on controlling the active power and reactive power of DFIG fed into the grid [26, 27], the results show that the min transition time is about 0.05s. Some research also has large fluctuating and significant overshoot [28, 29]. Therefore, with the proposed control system of DFIG applied the rotor sync signal method, the qualities of the shaft generator have improved significantly.

IV. THE POWER-SHARING SYSTEM OF SHIP GENERATOR STATION USING SHAFT GENERATOR

The shaft generator must connect to the ship grid and share the consumption load with the ship grid. There is some load-sharing method, for example, load-sharing based on the characteristic slope of Mechanic-Power, load-sharing based on the set- proportional. In this case, the author setups the load-sharing method based on the set-proportional shown in Figure 12. The division coefficient of active power is R_p, the division coefficient of reactive power is R_q. The active and reactive powers of the load are P_L and Q_L, respectively.

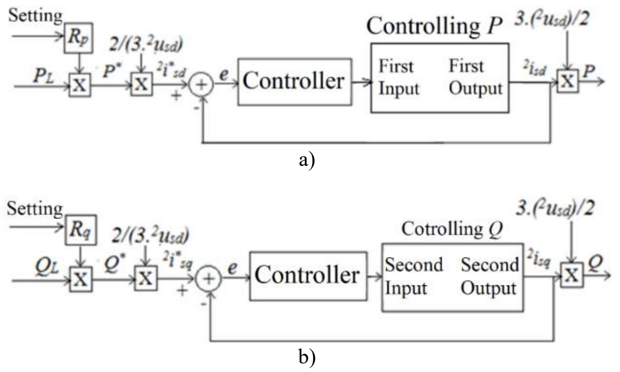

FIGURE 12. The power-sharing structure of shaft generator with the grid

The author tests the system as follows. Set the proportional $R_p=R_q=70\%$. In the initial time, connect the load with the active power $P_{L1}= 500kw$ and reactive power $Q_{L1}=300kvar$ to the grid. At the time of *1.5s*, add the second load with the active power $P_{L2}= 400kw$ and reactive power $Q_{L2}=0$. At the time of *1.6s*, add the third load with the active power $P_{L3}= 300kw$ and reactive power $Q_{L3}=300\ kvar$. At the time of 1.7s, cut the third load. At the time of 1.8s, cut the second load. The simulation results show in Figure 13.

The results show that the active and reactive powers of DFIG 2 fed into the grid always follow the desired values (70% power of the load) with a short transition time.

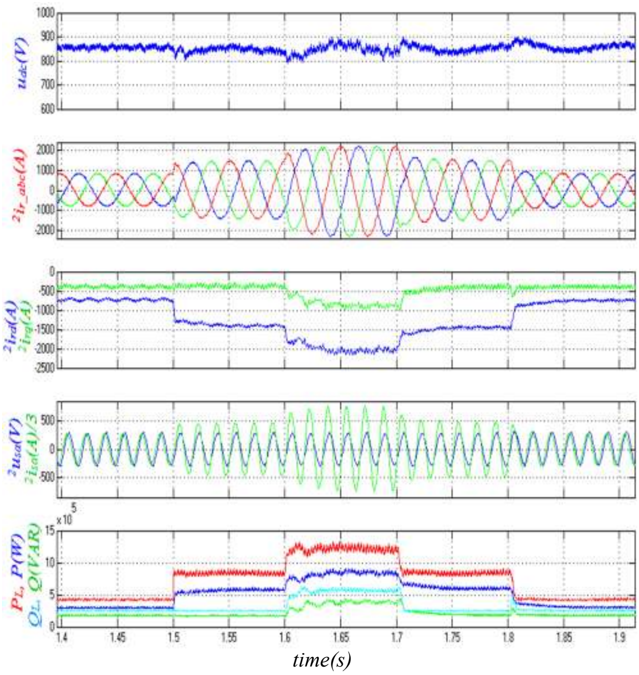

FIGURE 13. The power-sharing results

The above results are in the case of the loads with the constant active and reactive power. However, in practice, the power consumption of the load change usually and complexly. For example, the consumption of electric motors constantly changes according to the demand of motion. Therefore, to get realistic results, the author runs the system with another case as follows.

This article has been accepted for publication in a future issue of this journal, but has not been fully edited. Content may change prior to final publication. Citation information: DOI 10.1109/ACCESS.2021.3102659, IEEE Access

The load is the asynchronous electric motor which is the squirrel cage rotor (code 215HP, 320KW, 400V, 1487RPM). Initial time (before 1.5s), connect the electric motor to the grid, set the drag torque (T) on the motor shaft equals zero. Then, at 1.5s, the drag torque on the motor shaft equals 800 ($N.m$). Finally, at 1.9s, setting the motor shaft's drag torque equals 1600 ($N.m$). The results show in Figure 14.

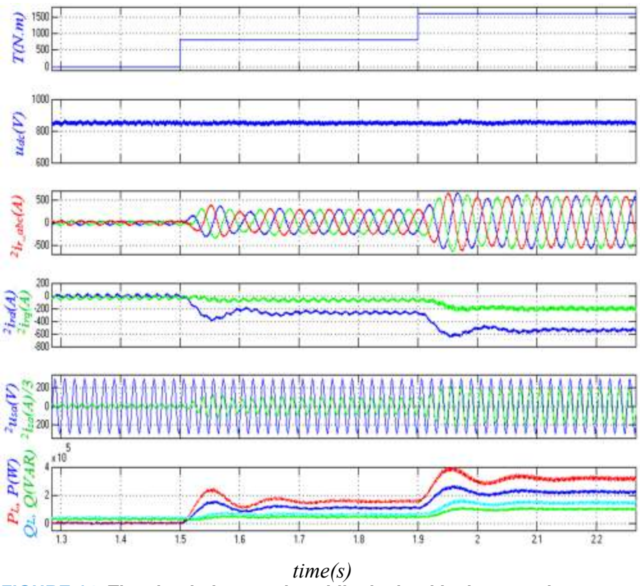

FIGURE 14. **The simulation results while the load is the asynchronous electric motor**

The results show that when drag torque on the motor shaft changes, the consumption of electric motor changes complexly, so the desired values of active and reactive power of shaft generator change complexly. However, the active and reactive power of the shaft generator fed into the grid always follows the desired values.

To more detail the ability to follow the desired values of the control system, we plot the expected values (70% power of the load) and the response values in the same graph shown in Figure 15. The results show that the response powers of the generator (P, Q) almost coincide with its desired values ($70\%P_L; 70\%Q_L$). Moreover, at the time of changing drag torque on the motor shaft ($t=1.5s; t=1.9s$), the current consumptions of the electric motor (i_{L_abc}) change rapidly, but the emit currents (${}^2i_{s\_abc}$) of the shaft generator also change immediately. Therefore, the emit current of the shaft generator change quickly and timely responds well to the load's consumption demand. This result contributes to ensuring the stability of the power grid on ships.

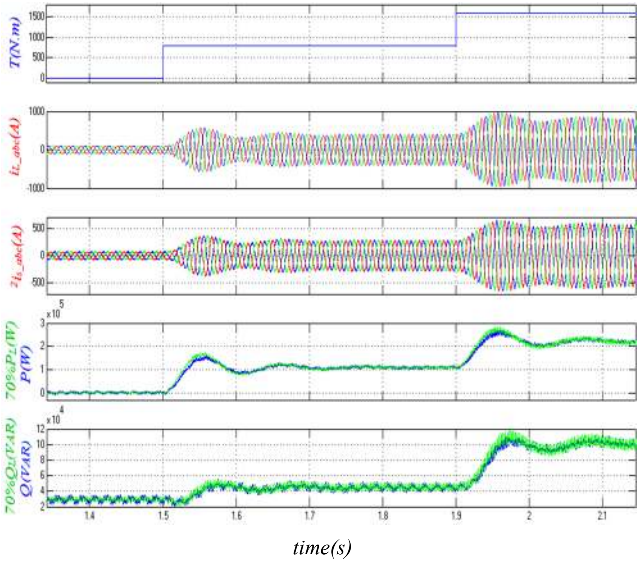

FIGURE 15. **The ability to follow the desired values of the control system while the load is an asynchronous electric motor**

V. CONCLUSION

The author has successfully built the ship's shaft generator system using DFIG with the rotor sync signal method. The control system structure is straightforward compared with the previous design. The proposed structure eliminates complicated coordinate conversion, so the manufacturing cost is cheaper. Besides, the proposed system has advantages such that the voltage of the generator is always equal to the grid's voltage in amplitude, frequency, and phase. Moreover, the system has a natural feature that the two control channels of active and reactive power are independent. Therefore, the system has met very well the requirements of power supply on ships such: the voltage of the generator always coincide with the voltage of the grid; the active and reactive power of the generator always follow the desired values with a short transition time, and none of the overshoot; the emitter current of shaft generator change quick and timely, response well the consumption demand of the load on the ship. In summary, the method's advantage is simple to control structure but high quality.

REFERENCES

[1] MAN B&W Diezel A/S, Shaft Generators for the MC and ME Engines, Denmark, 2004.

[2] Zhang, C., Cai, X., Molinas, M., & Rygg, A., "Frequency-domain modelling and stability analysis of a DFIG-based wind energy conversion system under non-compensated AC grids: impedance modelling effects and consequences on stability", *IET Power Electronics*, 2019, *12*(4), pp.907-914.

[3] Liu, J., Yao, W., Wen, J., Fang, J., Jiang, L., He, H., & Cheng, S., "Impact of power grid strength and PLL parameters on stability of grid-connected DFIG wind farm", *IEEE Transactions on Sustainable Energy*, 2019, *11*(1), pp.545-557.

[4] Kun Xia; Zhongwei Zhang; Nan Wang; Ping Zhang. Operation control and simulation research of the variable-speed constant-frequency system of the ship shaft generator. Presented at 2016 IEEE Region 10 Conference (TENCON), Singapore, 22-25 Nov. 2016; pp.301-304.

[5] Ju-ming Gao; Shan-ming Wan; Li-li Liu. The research of marine shaft generator system based on brushless doubly-fed machine.

Presented at 17th International Conference on Electrical Machines and Systems, Hangzhou, China, 22-25 Oct. 2014; pp.151-155.

[6] Li, P., Wang, J., Xiong, L., Huang, S., Wang, Z., & Ma, M., "SSCI mitigation of grid-connected DFIG wind turbines with fractional-order sliding mode controller", *Wind Energy*, 2020, *23*(7), pp.1564-1577.

[7] Wu, C., Cheng, P., Ye, Y., & Blaabjerg, F., "A Unified Power Control Method for Standalone and Grid-Connected DFIG-DC System" *IEEE Transactions on Power Electronics*, 2020, *35*(12), pp.12663-12667.

[8] Peng, L. ; Colas, F.; Francois, B. ; Li, Y. A modified vector control strategy for DFIG based wind turbines to ride-through voltage dips. In 2009 13th European Conference on Power Electronics and Applications, Barcelona, Spain, 8-10 Sept. 2009; pp. 1-10.

[9] Zhou, Y.; Bauer, P.; Ferreira, J. A.; Pierik, J. Operation of grid-connected DFIG under unbalanced grid voltage condition. *IEEE Transactions on Energy Conversion*, 2009, *24(1)*, pp.240-246.

[10] A. Tapia; G. Tapia; J. X. Ostolaza; J. R. Saenz. Modeling and control of a wind turbine driven doubly fed induction generator. *IEEE Trans. Energy Convers*, 2003, *18(2)*, pp.194–204.

[11] R. Cardenas; R. Pena; S. Alepuz; and G. Asher. Overview of Control Systems for the Operation of DFIGs in Wind Energy Applications. *IEEE Trans. Ind. Electron,* 2013, *60(7)*, pp.2776–2798.

[12] Nguyen, T. T., "A rotor-sync signal-based control system of a doubly-fed induction generator in the shaft generation of a ship", *Processes*, 2019, *7*(4), 188.

[13] Preindl, M., & Bolognani, S, "Model predictive direct speed control with finite control set of PMSM drive systems", *IEEE Transactions on Power Electronics*, 2012, 28(2), pp.1007-1015.

[14] Sun, X., Wu, M., Lei, G., Guo, Y., & Zhu, J. "An improved model predictive current control for PMSM drives based on current track circle", *IEEE Transactions on Industrial Electronics*, 2020, 68(5), pp.3782-3793.

[15] Sun, X., Cao, J., Lei, G., Guo, Y., & Zhu, J. "A robust deadbeat predictive controller with delay compensation based on composite sliding mode observer for PMSMs", *IEEE Transactions on Power Electronics*, 2021, 36(9), pp.10742-10752

[16] Sun, X., Hu, C., Lei, G., Guo, Y., & Zhu, J., "State feedback control for a PM hub motor based on gray wolf optimization algorithm", *IEEE Transactions on Power Electronics*, 2019, 35(1), pp.1136-1146.

[17] Yang, T., Sun, N., & Fang, Y., "Adaptive fuzzy control for a class of MIMO underactuated systems with plant uncertainties and actuator deadzones: Design and experiments", *IEEE Transactions on Cybernetics*, 2021.

[18] Yang, T., Sun, N., Chen, H., & Fang, Y., "Neural network-based adaptive antiswing control of an underactuated ship-mounted crane with roll motions and input dead zones", *IEEE Transactions on Neural Networks and Learning Systems*, 2019, 31(3), pp.901-914.

[19] Lavi, A., & Polge, R. J., "Induction motor speed control with static inverter in the rotor", *IEEE Transactions on Power Apparatus and Systems*, 1966, (1), pp.76-84.

[20] Xiao, S.; Geng, H.; Zhou, H.; Yang, G. Analysis of the control limit for rotor-side converter of doubly fed induction generator-based wind energy conversion system under various voltage dips. *IET Renewable Power Generation*, 2013, 7(1), pp.71-81.

[21] Rashid, M. M., and Ahmad Wali., "Fuzzy-PID hybrid controller for point-to-point (PTP) positioning system", *American Journal of Scientific Research*, 2010, pp.72-80.

[22] 15 [84] Sinthipsomboon, Kwanchai, "A hybrid of fuzzy and fuzzy self-tuning PID controller for servo electro-hydraulic system", *Industrial Electronics and Applications (ICIEA) 6th IEEE Conference on*, 2011, pp.220-225.

[23] Satish. R. V , Zafar. J. K," Performance of tuned PID controller and a new hybrid fuzzy PD + I controller", *World Journal of Modelling and Simulation, Vol. 6 No. 2*, pp.141-149.

[24] Hwang, H. S., Choi, J. N., Lee, W. H., & Kim, J. K.," A tuning algorithm for the PID controller utilizing fuzzy theory", *Neural Networks 1999-IJCNN'99. International Joint Conference on,* 1999, *Vol.4*, pp.2210-2215.

[25] Xu, J., & Feng, X.," design of adaptive fuzzy PID tuner using optimization method", *Intelligent Control and Automation, 2004-WCICA 2004. Fifth World Congress on*, 2004, *Vol. 3,* pp.2454-2458.

[26] Jang, J. I., Kim, Y. S., & Lee, D. C.," Active and reactive power control of DFIG for wind energy conversion under unbalanced grid voltage", *Power Electronics and Motion Control Conference 2006-IPEMC2006. CES/IEEE 5th International*, 2006, *Vol. 3*, pp.1-5.

[27] Hu, J., Nian, H., Hu, B., He, Y., & Zhu, Z. Q," Direct active and reactive power regulation of DFIG using sliding-mode control approach", *Energy Conversion, IEEE Transactions* on, 2010, *VoL.25, No.4*, pp.1028-1039.

[28] Sun, L., Mi, Z., Yu, Y., Wu, T., & Tian, H.," Active power and reactive power regulation capacity study of DFIG wind turbine" *Sustainable Power Generation and Supply 2009-SUPERGEN'09, IEEE International Conference on,* 2009, pp.1-6.

[29] Mishra, J. P., Hore, D., & Rahman, A.," Fuzzy logic based improved Active and Reactive Power control operation of DFIG for Wind Power Generation", *Power Electronics and ECCE Asia (ICPE & ECCE), 2011 IEEE 8th International Conference on*, (2011), pp.654-661.